C5orf30 is a negative regulator of tissue damage in rheumatoid arthritis

Munitta Muthana[a,1], Sarah Hawtree[a], Adam Wilshaw[a], Eimear Linehan[b], Hannah Roberts[a], Sachin Khetan[a], Gbadebo Adeleke[a], Fiona Wright[a], Mohammed Akil[a], Ursula Fearon[b], Douglas Veale[b], Barbara Ciani[c], and Anthony G. Wilson[a,b]

[a]Academic Unit of Rheumatology, University of Sheffield, Sheffield S10 2RX, United Kingdom; [b]Department of Rheumatology, Dublin Academic Medical Centre and the Conway Institute of Biomolecular and Biomedical Research, University College Dublin, Dublin D04 W6F6, Ireland; and [c]Centre for Membrane Interactions and Dynamics, and Krebs Institute, Department of Chemistry, University of Sheffield, Sheffield S3 7HF, United Kingdom

Edited by Arthur Weiss, University of California, San Francisco, CA, and approved July 31, 2015 (received for review March 12, 2015)

The variant rs26232, in the first intron of the chromosome 5 open reading frame 30 (*C5orf30*) locus, has recently been associated with both risk of developing rheumatoid arthritis (RA) and severity of tissue damage. The biological activities of human C5orf30 are unknown, and neither the gene nor protein show significant homology to any other characterized human sequences. The C5orf30 gene is present only in vertebrate genomes with a high degree of conservation, implying a central function in these organisms. Here, we report that C5orf30 is highly expressed in the synovium of RA patients compared with control synovial tissue, and that it is predominately expressed by synovial fibroblast (RASF) and macrophages in the lining and sublining layer of the tissue. These cells play a central role in the initiation and perpetuation of RA and are implicated in cartilage destruction. RASFs lacking C5orf30 exhibit increased cell migration and invasion in vitro, and gene profiling following C5orf30 inhibition confirmed up-regulation of genes involved in cell migration, adhesion, angiogenesis, and immune and inflammatory pathways. Importantly, loss of C5orf30 contributes to the pathology of inflammatory arthritis in vivo, because inhibition of C5orf30 in the collagen-induced arthritis model markedly accentuated joint inflammation and tissue damage. Our study reveal C5orf30 to be a previously unidentified negative regulator of tissue damage in RA, and this protein may act by modulating the autoaggressive phenotype that is characteristic of RASFs.

rheumatoid arthritis | genetics | inflammation | tissue damage | fibroblast

Rheumatoid arthritis is a chronic systemic autoimmune disease characterized by a symmetrical, inflammatory arthropathy that frequently results in damage to synovial-lined joints with consequent pain, stiffness, and reduced functional capacity. The prevalence of RA is 0.8–1% in Western Europe and North America, and it is believed to arise from an interplay between genetics and the environment. Smoking is known to be a major risk factor particularly for anticitrullinated protein antibody-positive RA (1), whereas consumption of alcohol reduces both the risk and the severity of RA (2). The severity of RA varies from a mild condition with little joint damage to an unremitting condition that leads to extensive bone and cartilage damage. The radiological severity of damage to the hands and feet is widely used to measure outcome of RA and has been shown to have a significant genetic component (3, 4). Loci genetically associated with radiological damage include *DRB1* (5), *CD40* (6) and *TRAF1/C5* (7), *IL-4* (8), and *IL-15* (9).

A genome-wide association study involving 12,277 RA cases and 28,975 controls, all of European descent, reported association of rs26232 in the first intron of chromosome 5 open reading frame 30 (*C5orf30*) with risk of RA (10). Importantly linkage disequilibrium did not extend to genes in the flanking regions, indicating that the association was arising from *C5orf30*. This association was subsequently replicated in a British study of 6,108 RA cases and 13,009 controls (11). In a study of three large European RA populations (n = 1,884), we reported an allele dose association of rs26232 with radiological damage (12).

The biological activities of human C5orf30 are unknown, and the precise roles it plays in RA have not yet been reported. There is indirect evidence linking human C5orf30 with immune function via its association with intracellular UNC119 (13); the latter increasing both T-cell activation by up-regulating Lck/Fyn activity and Src kinases regulating macrophages activation (14, 15). There are, however, no studies of the biological functions of human C5orf30 and, in view of the genetic association with RA susceptibility and severity, we have undertaken in silico analysis and both in vitro and in vivo experiments to determine its functional activities in RA. Here, we report C5orf30 to be a yet unidentified negative regulator of tissue damage in RA, acting by modulating the autoaggressive phenotype that is characteristic of RA synovial fibroblasts (RASF). It is highly expressed in the synovium of RA patients compared with healthy and osteoarthritis (OA) predominately by RASF in the lining and sublining layer. These cells play an important role in the initiation and perpetuation of RA and are implicated in cartilage destruction (16). Targeting C5orf30 expression by using siRNA technology resulted in increased invasiveness, proliferation and migration of RASFs in vitro, and modulated expression of genes in RA-relevant pathways including migration and adhesion. Importantly, loss of C5orf30 contributes to the pathology of inflammatory arthritis in vivo, because inhibition of C5orf30 in the collagen-induced arthritis (CIA) model

Significance

Recent studies have reported genetic association of chromosome 5 open reading frame 30 (*C5orf30*) with both rheumatoid arthritis (RA) susceptibility and the severity of radiological damage to joints. The gene is expressed in vertebrate genomes with a high degree of conservation, implying a central function in these organisms. Here, we report that C5orf30 encodes a 206-aa protein that is highly expressed in RA synovial fibroblasts (RASFs), a cell type implicated in causing joint damage. Importantly inhibition of C5orf30 increases the autoaggressive phenotype of RASFs in vitro and increases joint inflammation and damage in murine inflammatory arthritis. Our data reveals C5orf30 to be a negative regulator of tissue breakdown modulating the autoaggressive phenotype that is characteristic of RASFs.

Author contributions: M.M. and A.G.W. designed research; M.M., S.H., A.W., E.L., H.R., S.K., G.A., F.W., U.F., and B.C. performed research; M.A. and D.V. contributed new reagents/analytic tools; M.M., E.L., U.F., B.C., and A.G.W. analyzed data; and M.M. and A.G.W. wrote the paper.

The authors declare no conflict of interest.

This article is a PNAS Direct Submission.

Data deposition: The microarray data reported in this paper have been deposited in the Gene Expression Omnibus (GEO) database (accession no. GSE72258).

[1]To whom correspondence should be addressed. Email: m.muthana@shef.ac.uk.

This article contains supporting information online at www.pnas.org/lookup/suppl/doi:10.1073/pnas.1501947112/-/DCSupplemental.

mice markedly accentuated joint inflammation and cartilage destruction. These data confirm C5orf30 as a previously unidentified regulator of tissue destruction in RA.

Results

Phylogeny and Structure of C5orf30. The *C5orf30* locus is located on chromosome 5 (102,595,125–102,614,361 bp), the three exons encode a protein of 206 aa. We used the PhylomeDB database (17) to analyze the evolution of *C5orf30*-related sequences (www.phylomedb.org). Strikingly, single *C5orf30* orthologs were found only in vertebrates, where the protein sequences show a high degree of conservation, such as in chimpanzee (99.5%), mice (94%), and chicken (89%) with the most distant ortholog found in bony fish (72% identity to human sequence) (Fig. 1*A* and Fig. S1). C5orf30 protein amino acid sequences do not show significant homology to any characterized protein or structure, making 3D structure prediction unreliable. Nonetheless, secondary structure and globular domain predictions performed by using Jpred3 and GlobPlot (18, 19) indicate the C5orf30 polypeptide sequence is likely to adopt regions of mixed α-helical and β-sheet structure, within a likely folded domain between amino acids 43 and 110 (Fig. 1*B*). To glean more information on the potential biological roles of C5orf30, the Eukaryotic Linear Motif database was used to search for regulatory regions of the human C5orf30 protein sequence that may also be involved in binding to accessory proteins (20). One peculiar feature identified in all C5orf30 protein sequences is a poly-arginine stretch (Fig. 1*B*) followed by serine residues. This amino acid motif matches the consensus sequence for the basophilic AGC kinases (such as protein kinase B), which regulate cell migration and whose activity is stimulated by integrin binding and interaction with T-cell receptors (21). C5orf30 sequences also contains a motif matching closely the consensus for CDK1 phosphorylation (amino acids 20–30), which coupled to recognition sequences for cyclins (amino acids 139–170) is a strong indication of a roles for C5orf30 in the cell cycle. C5orf30 encodes a basic polypeptide (pI 9.5), a feature typical of proteins interacting with phospholipids, membranes, and/or nucleic acid interactions. Roles in membrane transport are further supported by the presence of a potential LC3-interacting region (amino acids 167–173), which is necessary for binding to the autophagy machinery. C5orf30 contains a predicted nuclear export sequence (amino acids 184–198), nonetheless, the protein does not contain a standard nuclear import sequence, suggesting that posttranslational modifications or binding to a chaperone protein are necessary for C5orf30 import into the nucleus (Fig. 1*B*). Ultimately, we mined the RegulomeDB database to identify regulatory elements in noncoding regions of the human C5orf30 potentially affected by the RA-associated rs26232 SNP in the first intron of this gene (18). The ENCODE analysis indicate that this SNP is likely to affect the binding site for several transcription factors, of particular interest, USF2, required for the hypoxic transcriptional response and the activation of HIF genes (22), and BHLHE40, a regulator of chondrogenesis.

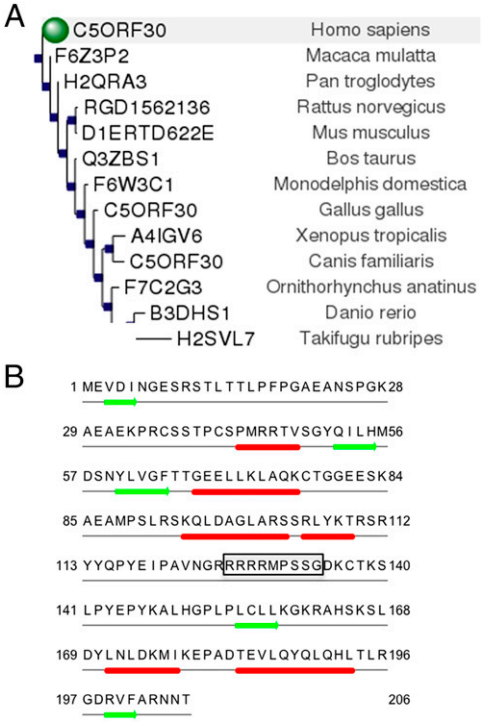

Fig. 1. Phylogeny and structure of C5orf30. (*A*) Maximum likelihood (ML) tree of *C5orf30* generated using the human sequence as seed and a JTT evolutionary model by PhylomeDB. C5orf30 is set as an arbitrary root in the image. The tree shows identified orthologs by speciation events (blue nodes). The scale-bar for branch length is indicated. (*B*) Jpred secondary structure prediction for human C5orf30; box indicates poly-arginine stretch followed by serine residues (red cylinders, α-helices; green arrows, β-sheets).

Tissue-Specific Expression of C5orf30 in RA. We measured C5orf30 mRNA expression in a panel of human cell lines and tissues. Human peripheral blood leukocytes (PBLs) from healthy individuals expressed high levels of C5orf30 mRNA particularly myeloid-derived cells compared with lymphocytes (B and T cells) and other cell lines (Fig. 2*A*). RASF had the highest levels of C5orf30 mRNA, significantly greater than in OASF ($P = 0.001$). Interestingly, C5orf30 expression in PBLs from RA patients ($n = 117$) was significantly lower (0.5-fold) than in healthy donors ($n = 107$) (Fig. 2*B*). However, we cannot be sure that this finding is not due to a different peripheral blood leukocyte composition between the two groups. Immunohistochemistry staining revealed significant expression of C5orf30 protein throughout the RA tissue section (Fig. 2*C*) and was predominantly located in the lining and sublining layer of the synovium with little or no expression detected in the synovium obtained from healthy controls or osteoarthritis (OA) patients (Fig. 2 *C–E*). Immunofluorescence staining of sections of the RA synovium revealed C5orf30 colocalized with synovial fibroblast and synovial macrophages (Fig. 2*F*); however, expression was considerably lower in endothelial cells and both B and T lymphocytes (Fig. 2*G*).

Modulation of C5orf30 Expression in RASF. Given that RA synovial fibroblasts express C5orf30 (Fig. 2*A*), we investigated whether its expression is modulated in response to conditions experienced in RA joints including high levels of the inflammatory cytokine tumor necrosis factor (TNF) (23) and low oxygen tension (24). We investigated expression of C5orf30 at all of the different passages used in this study and found no significant difference in expression from passages 3–8 (Fig. S2*A*). RASF were treated for 4 h with TNF (50 ng/mL), hypoxia (0.5% O_2), and a combination of TNF and hypoxia. Cell viability was assessed by flow cytometry and was not affected by these culture conditions (Fig. S2*B*). Cultured RASF exposed to hypoxia consistently up-regulated C5orf30 mRNA (eightfold) compared with untreated cells (Fig. 3*A*), whereas incubation TNF had the opposite effect (0.5-fold) ($P = 0.008$). The effect of TNF overrides that of hypoxia at both the mRNA and protein level (Fig. 3 *A* and *B*).

C5orf30 Knockdown Regulates RASF-Related Pathology. The biological effects of C5orf30 inhibition ($C5orf30^{KD}$) in RASFs were investigated by using 50 nM anti-C5orf30 siRNA or 50 nM nontargeting (NTC) siRNA. The former treatment resulted in a 70% reduction in C5orf30 mRNA and protein expression at 24 and 48 h (Fig. S3 *A–C*). RASF depleted of C5orf30 did not induce cell

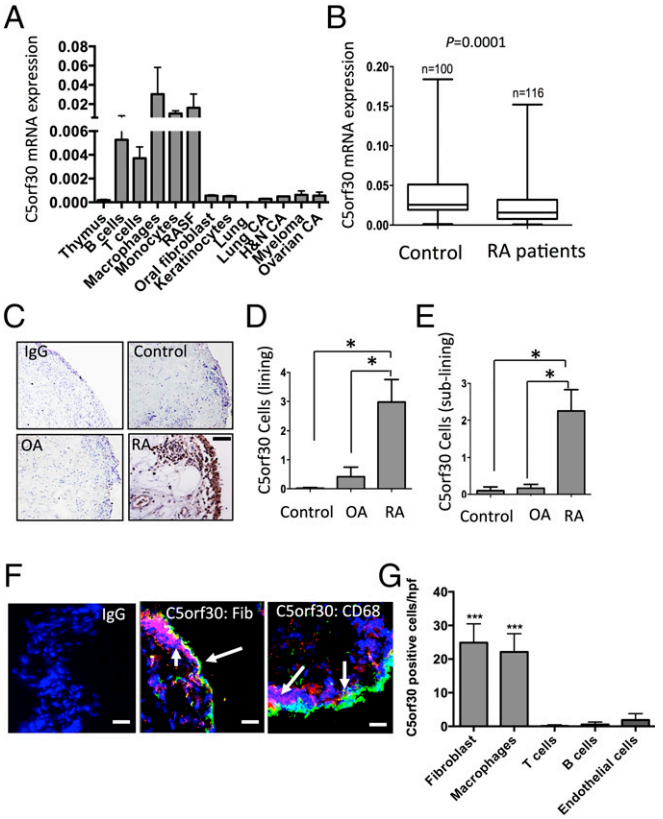

Fig. 2. Tissue specific expression of C5orf30 in RA. C5orf30 mRNA expression in human tissues and cell lines are greater in RASF and myeloid derived cells from healthy volunteers (*A*). Quantitative expression of *C5orf30* mRNA was detected at lower levels in PBLs from RA patients (n = 116) compared with healthy controls from the general population (n = 100). Individual results are expressed as the means and SEM of duplicate determinations (*B*). Immunohistochemistry reveals tissue-specific C5orf30 expression (*C*) in the synovial lining (*D*) and sublining layer (*E*). n = 5 control; n = 6 OA and RA. (*F*) C5orf30 colocalization with synoviocytes. The white arrows point to areas of colocalization (yellow) of *C5orf30* (red) with RASF (green) surface protein or CD68-expressing macrophages (green). Colocalization was not evident with other cell types (*G*). (Scale bars: *C*, 100 μm; *E*, 50 μm.) n = 5 patients per group. *P < 0.05, **P < 0.01, ***P < 0.001.

death compared with control cells as assessed by flow cytometry (1.6 ± 0.5% vs. 2.1 ± 0.5%, n = 5, respectively), nor did it influence cell proliferation (Fig. S4*B*). We therefore sought to determine whether C5orf30^{KD} influenced cell migration and invasion, which are characteristic of RASFs. As shown in Fig. 3*C*, C5orf30^{KD} significantly increased the number of migrating RASFs compared with NTC^{KD} in a scratch/wound assay, leading to faster closure of the wound by 24 h (n = 6, $P \leq 0.02$; NTC^{KD} 51.2 ± 4.5% vs. C5orf30^{KD} 60.4 ± 4.6%). Similarly, C5orf30^{KD} significantly increased RASF invasion through Matrigel over a 24-h period by 40%, compared with controls (n = 6, $P \leq 0.0031$; NTC^{KD} 5.7 ± 0.9% vs. C5orf30^{KD} 15.6 ± 3.2%) (Fig. 3*D*). Together these results strongly suggest that C5orf30 has a fundamental regulatory role in RASF migration and invasion. We then determined the effects of C5orf30^{KD} on global gene expression; RASF from three patients were subjected to C5orf30^{KD} or NTC^{KD} and Illumina BeadChip arrays revealed >990 differentially expressed genes (DEGs) between the two groups with $P < 0.05$ using integrative statistical testing. A volcano plot depicting the significant differences ($P < 0.05$) in expression patterns between the NTC^{KD} and C5orf30^{KD} group are shown, where the red dots represent a difference in expression patterns between the two groups (Fig. 3*E*).

Although many of the differentially expressed genes were unknown or hypothetical genes, 111 of the genes that were affected by C5orf30^{KD} have been related to arthritis and include cytokines, matrix proteins, inflammation, and cell adhesion and migration (Fig. 3*F*) (25–29). Selected genes modulated by C5orf30^{KD} are shown in Table S1. Confirmation of the microarray data with quantitative RT-PCR (qRT-PCR) was performed for selected genes (Fig. S5). C5orf30 was also overexpressed by transfecting RASF with a pCMV6-Entry Vector containing the ORF of C5orf30 resulting in >300-fold mRNA expression of C5orf30 compared with mock-transfected cells (Fig. S6*A*) and was also confirmed at the protein level by Western blotting (Fig. S6*B*). C5orf30 overexpression on genes known to previously affected by C5orf30^{KD} (Fig. S5) was assessed by real-time PCR. Interestingly, some of the genes that were up-regulated with C5orf30^{KD} were significantly down-regulated in response to C5orf30 overexpression (CYR61, CXCL6, COL1A, and CD44). Genes that were down-regulated with C5orf30^{KD} were greatly up-regulated (CXCL3 and TSPAN2) (Fig. S6*C*).

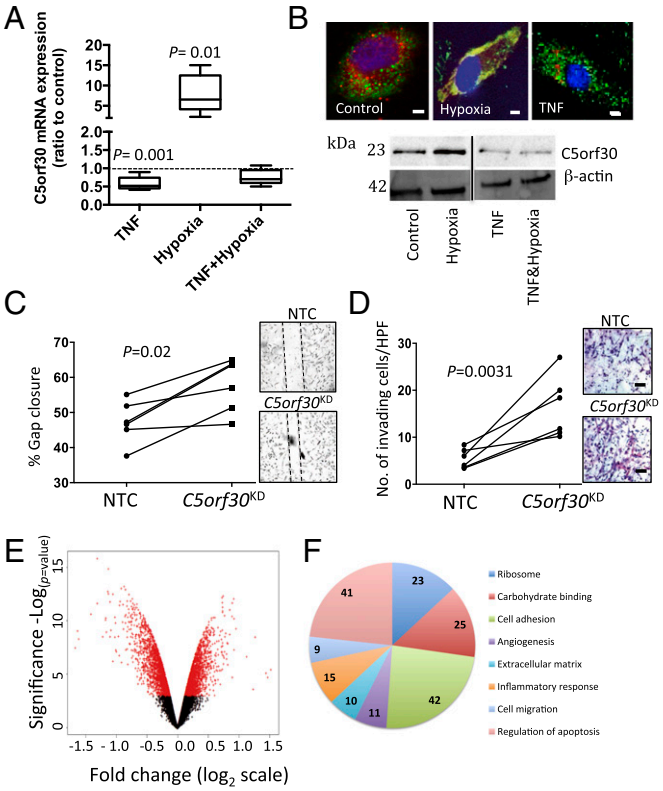

Fig. 3. C5orf30 modulates the autoagressive phenotype of RASF. (*A*) *C5orf30* mRNA expression in the TNF and hypoxia-treated samples are expressed relative to control untreated RASF (*A*). Hypoxia consistently induced an increased level of mRNA expression. TNF treatment reduced expression (0.5-fold), as did a combination of both TNF and hypoxia. n = 5 patients, and the data are represented as mean ± 95% confidence interval (dotted line represents change from untreated cells). This finding was confirmed by immunofluorescence (red, anti-*C5orf30*; blue, DAPI; green, LAMP-1) and Western blots (*B*). Protein lysates were collected from treated RASF, run on a Western blot, and probed for C5orf30 expression, using β-actin expression as a control. (The black line indicates discontinuous bands.) (*B*). In *C5orf30*^{KD} studies, RASF were treated with 50 nM anti-*C5orf30* siRNA or nontargeting (NTC) siRNA. *C5orf30*^{KD} increased cell migration (*C*) and invasion compared with the NTC (*D*). Data are from n = 6 RASF donors. Volcano plot of microarray data are presented (*E*) and a pie chart showing differentially expressed genes based on cluster analysis (*F*). (Scale bars: 100 μm.)

Inhibition of C5orf30 Drives Inflammation and Tissue Damage in CIA. Having established C5orf30 as a negative regulator of RASF invasion and migration, we hypothesized that C5orf30^{KD} might drive pathology in CIA. To test this hypothesis, mice were administered three doses of 5 mg/kg C5orf30 or NTC siRNA via tail vein injection (30). C5orf30^{KD} was confirmed in the paws of mice 72 h after administration by qRT-PCR (Fig. S7*A*). Mice were monitored daily; paw inflammation developed in all collagen-treated animals after 4 wk and became increasingly pronounced by week 7 (Fig. 4*A*), C5orf30^{KD} markedly exacerbated paw inflammation that was statistically significant by week 6 (Fig. 4 *A* and *B*). Three-dimensional microcomputed tomography imaging revealed the extent of bone erosion in hind paws of representative mice (Fig. 4*B* and Fig. S7*B*), and unlike all of the other groups, hind paws of C5orf30^{KD} mice exhibited severe loss of bone density and bone volume in the metatarsal region (Fig. 4*C* and Fig. S7*C*), demonstrating a key role for C5orf30 in modulating joint damage. Furthermore, histological analysis of the ankle joints of these mice showed significantly increased synovial inflammation and hyperplasia, formation of pannus tissue, and cartilage destruction compared with tissue sections of all of the other groups of mice (Fig. 4 *C*–*E* and Fig. S7*C*). The increase in inflammatory cytokines such as TNF and IL-1 and the down-regulation of antiinflammatory IL-10 in the mouse joints following C5orf30^{KD} indicates an important role in regulating inflammatory cytokine networks in inflammatory joint disease (Fig. 4*F*). Interestingly, the expression of C5orf30 in the front and hind paw joints at the end of the CIA study (day 49) increased significantly (front paws $P < 0.001$, hind paws $P = 0.0061$) in the C5orf30^{KD} compared with NTC-treated mice (Fig. S8), possibly due to the loss of siRNA-mediated inhibition.

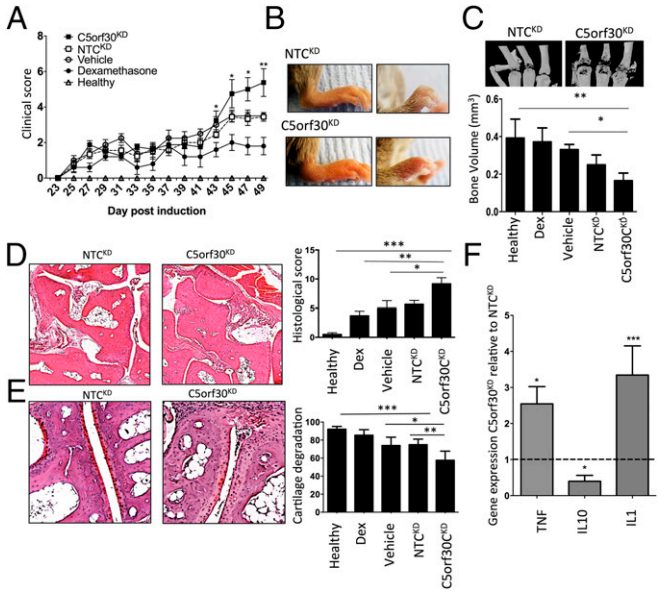

Fig. 4. *C5orf30^{KD}* augments CIA. Mice were treated with C5orf30 siRNA, NTC siRNA (5 mg/kg), or transfection reagent (vehicle) $n = 10$ mice per group. A group of mice also received Dexamethasone (Dex) (0.5 mg/kg). *C5orf30^{KD}* significantly increased arthritis (*A*). Representative front and hind paw images of CIA in mice treated with NTC or C5orf30 siRNA (*B*). At day 49, joint disease was assessed by MicroCT (*C*), H&E (*D*), and Safranin O (*E*). Analysis of *C5orf30^{KD}* was performed byusing a one-way ANOVA with multiple comparisons (*$P < 0.05$, **$P < 0.01$, ***$P < 0.001$). qRT-PCR of hind paws shows the relative mRNA expression of genes in the paws of *C5orf30^{KD}* compared with NTC treated mice (*F*).

Discussion

In this study, we implicate C5orf30 as a previously unidentified regulator of tissue destruction in RA. The RASF is a central mediator of tissue destruction typified by a semitransformed phenotype in vitro with loss of contact inhibition, high proliferative activity, resistance to apoptosis and production of chemokines, adhesion molecules, and proteases (31). Using in vitro assays, we show that C5orf30^{KD} enhances this autoaggressive phenotype including invasiveness and migration. As expected, based on the results from the RASF experiments, C5orf30^{KD} resulted in exacerbation of both joint inflammation and damage in the CIA model. A particularly notable finding is up-regulation of the proinflammatory cytokines TNF and IL-1 and down-regulation of IL-10 in joint tissue, potentially a consequence of expression by nonstromal cells, probably myeloid, which are the major source of TNF in inflamed joints.

C5orf30 is a strongly conserved gene from human to euteleostomi, the clade including the bony vertebrates. It is curious that this gene codes highly conserved protein sequences from bony fish through primates, indicating a major specialized function in vertebrates. Currently, the only known binding partner of C5orf30 is unliganded UNC119 (13), a transporter of myristoylated proteins to the primary cilia in photoreceptor and sensory cells (32). C5orf30 shows a punctate cytoplasmic vesicular distribution in RASF (Fig. 3*B*), suggesting a link to membrane trafficking. This link is further strengthened by the microarray data revealing genes affected by C5orf30 depletion in RASFs such as ARL6IP1, a transmembrane protein involved in membrane protein transport in hematopoietic cells (33); and ERC1, a Rab6 endosomes-interacting protein essential for cell migration and adhesion turnover (34). C5orf30 proteins do not show any similarity to any characterized protein sequence, making impossible the inference of its cellular function from homology; nonetheless, their amino acid composition makes them positively charged at physiological conditions, suggesting that natural interacting partners are negatively charged molecules, such as lipids or phosphorylated cargo. Human and mouse C5orf30 are phosphorylated at multiple sites, as revealed by multiple high-throughput proteomic studies (www.phosphosite.org). The occurrence of widespread phosphorylation may be considered as a means of regulating interactions with binding partners by modulation of the protein pK_a.

Interestingly, data provided from the ENCODE project suggest that the RA-associated rs26232 SNP is located in a regulatory region involved in the binding of several transcription factors associated with cell-cycle regulation, cell differentiation, the hypoxic transcriptional response, and chondrogenesis. Biological activities consistent with the pathways defined by the genes modulated by C5orf30 depletion therefore, taken together with the data collected in silico, in vitro, and in vivo provide evidence that link C5orf30 to membrane trafficking, the regulation of cell migration, and the cell cycle.

Interestingly, C5orf30 expression in PBLs from RA patients was significantly lower than in healthy cases, which may be due to the high background levels of TNF, a pivotal inflammatory mediator in this condition. In our study, we did not find an association between rs26232 genotype and C5orf30 mRNA levels in RA cases or controls, nor did a study of monocytes (35). Variability in expression of C5orf30 3′untranslated (UT) mRNA has been associated with rs26232 genotype (36), and variability in 3′UT sequences can, by influencing mRNA-protein scaffolds, result in differences in intracellular localization of proteins (37). This genotype–phenotype association may be the underlying mechanism explaining the link of rs26232 with severity of tissue damage in RA, however this hypothesis will need to be proven experimentally.

Cells in the rheumatoid joint are exposed to both hypoxia and high TNF levels; our results reveal contrasting effects on C5orf30

expression with TNF having a dominant negative effect that may contribute to the catabolic activities of this cytokine in RA. There is evidence of immune abnormalities that predate the clinical onset of RA symptoms (38); during this period RA risk loci are thought to be involved in the process of loss of immune tolerance and development of subclinical abnormalities. This preclinical phase is likely to involve nonjoint tissue such as the lung or lymph nodes (39). It is likely that loci associated with severity of joint damage, such as C5orf30, are expressed within the inflamed synovial tissue and regulate pathways involved in tissue damage.

The vast majority of RA susceptibility loci identified in recent genome-wide associations studies in RA are involved in the immune system, particularly implicating regulatory and memory T cells, and NF-κB and JAK-STAT signaling pathways (40). In contrast, C5orf30 is not expressed at significant levels in lymphoid cell lines or RA synovial lymphocytes, but is present in the two cell types, myeloid and stromal, implicated in mediating tissue destruction in RA. Macrophages are present in large numbers in the RA synovium and are responsible for the secretion of proinflammatory mediators, such as TNF and IL-6, that can activate RASFs. Although our studies implicate C5orf30 in the autoaggressive phenotype of RASFs, it may also regulate the tissue damaging activities of RA synovial macrophages and this possibility will need to be explored in future studies.

Methods

Phylogeny and Structure of *C5orf30*. BLAST was used for the initial homology search against the nonredundant proteins database (nr), using the BLOSUM62 matrix and default parameters. Only sequences with E value higher than the default threshold (PSI-BLAST threshold 0.005) were included in a PSI-BLAST iterative search, which was continued until no new *C5orf30* sequences were found (convergence).

C5orf30 mRNA Levels in Leukocytes. Peripheral blood samples were obtained from 314 healthy individuals and 281 RA patients as described (41). The diagnosis of RA was based on the 1987 American College of Rheumatology criteria. Approval was obtained from the South Sheffield Research Ethics Committees, and informed consent was obtained from all participants. Whole blood was collected into QIAGEN PAXgene tubes (QIAGEN), and total RNA was extracted according to the PAXgene RNA system and quantitated by using Ribogreen reagent (Molecular Probes). Total RNA was reverse-transcribed by using *ImpromII* reverse transcriptase and random primers (Promega). PBL were also isolated from platelet-depleted buffy coats (Blood Transfusion Service) by using the human B and T-cell RosetteSep enrichment kits (StemCell Technologies) and Ficoll-Paque Plus (Amersham Pharmacia) as described by us (42).

Synovial Tissue Samples. Samples for immunohistochemistry and confocal microscopy were obtained from knee joints of RA ($n = 20$) and OA ($n = 6$) and healthy donors ($n = 5$) recruited at the Royal Hallamshire Hospital and St. Vincent's University Hospital, and ethical permission was obtained from the Medical Research Ethics Committee in accordance with the Declaration of Helsinki principles. Briefly, arthroscopy and synovial biopsy was performed, under local anesthesia and sterile conditions, using a Storz 2.7-mm needle arthroscope (Storz) and a 2-mm grasping forceps. Biopsy samples were obtained from all compartments of the knee joint, embedded in Tissue-Tek OCT compound (Sakura Finetek), snap frozen, and stored in liquid nitrogen until for immunofluorescence staining. Alternatively tissue was embedded in paraffin wax for histological labeling studies.

Isolation and Culture of RASF. Fresh synovial biopsies were digested by using 1 mg/mL collagenase type 1 (Worthington Biochemical). Dissociated cells were grown to confluence (10 d) in RPMI 1640 medium (Lonza) , 10% (vol/vol) FCS (Invitrogen), penicillin (100 units/mL), streptomycin (100 units/mL) before trypsinization and passage. This was the optimum condition for culture of RASFs. Passages 3–8 of the RASF were used in subsequent experiments, at which time they were a homogeneous population of fibroblasts. Before each experiment, the RASF were serum-starved for 24 h in DMEM. To study the effect of RA-like conditions, RASF were either subjected to severe hypoxia (<0.5% O_2) in a humidified multigas incubator (Heto) or treated with 50 ng/mL TNF (Peprotech) for 4 h in a normoxic environment [20.9% (vol/vol) O_2] in 5% (vol/vol) CO_2. In some experiments, 50 ng/mL TNF was added to RASF and placed in the hypoxic incubator. For controls, RASF were untreated and incubated at 37 °C with 5% CO_2 for 4 h. The effect on C5orf30 expression following such treatments was assessed by real-time PCR, fluorescence microscopy. Cell death was assessed by flow cytometry by using a FITC Annexin V/Dead Cell Apoptosis Kit (Thermo Fisher Scientific).

Real-Time PCR. Total mRNA was extracted from cultured RASF (1×10^6 cells) or mouse tissues by using the RNeasy Mini Kit (QIAGEN). Reverse transcription of 2 μg of total mRNA was carried out at 42 °C by using the SuperScript Reverse Transcription system (Primer Design). For murine bones, RNA extraction was performed by using TRIzol. PCR amplification of cDNA (aliquot) was performed by adding 2.5 nM dNTPs, 2.5 units of Taq DNA polymerase (Primer design), and 0.25 μM sense and antisense primers. The reaction took place in 25 μL of PCR buffer, consisting of 1.5 mM $MgCl_2$, 50 mM KCl, and 10 mM Tris·HCl (pH 8.3). To measure the levels of *C5orf30* mRNA, the following primer pairs were used 5′-AGGACCGTGTCAGGCTACC-3′ (sense) and 5′-TGTTTGGAGCGTAAGGATGGC-3′ (antisense) for murine C5orf30 sequence – TGAGATCCCAGCGGTTAATGG (sense).

Reverse – GGAGTGAGCCCTCTTACCTTT (antisense). Housekeeping genes included β-actin, 5′-GGA CTT CGA GCA AGA GAT GG-3′ (sense) and 5′-TGT GTT GGG GTA CAG GTC TTT G-3′ (antisense), and GAPDH 5′-ACC ACA GTC CAT GCC ATC AC-3′ (sense) and 5′-TCC ACC ACC CTG TTG CTG TA-3′ (antisense). Add murine housekeeping genes. Reactions were processed in a DNA thermal cycler (ABI Prism 7900HT Sequence Detection System, Life Technologies) with 50 cycles of 15 s of denaturation at 95 °C, and 60 s of annealing at 60 °C, followed by 50 s of elongation at 72 °C. The Ct values generated from these samples were normalized to a housekeeping gene. To calculate the absolute concentration of *C5orf30* in the sample, a standard curve was created by using a serial dilution of a *C5orf30* plasmid clone (BioScience) at a known concentration of 227.76 ng/μL. A standard curve was created by using Microsoft Excel, and a line equation for the *C5orf30* standard curve was $y = -1.759\ln(x) + 9.745$. This equation was used to convert all of the Ct values in the study to absolute concentrations.

Immunohistology. Tissue obtained at arthroscopy from the knees of individuals with RA was fixed in 10% (vol/vol) neutral buffered formalin and embedded in paraffin wax. Sections (5 μm) were mounted onto glass slides, and antigen retrieval was achieved by heating in trisodium citrate (pH 6.0) for 10 min in a high-powered microwave. A C5orf30 peptide affinity-purified rabbit polyclonal antibody (PAb) (Sigma) was added to the slides (1:50), which were incubated at 4 °C overnight. Controls were incubated in the same dilution of matched IgG1. Bound antibody was detected by using an avidin–biotin–complex (ABC) peroxidase kit (Vector). Briefly, 50 μL of biotinylated goat anti-secondary antibody was added for 30 min, then ABC peroxidase was added for a further 30 min. Peroxidase activity was then measured by using a 3,3-diaminobenzidine substrate. All slides were counterstained with Gills hematoxylin.

C5orf30 siRNA-Mediated Knockdown. To compare the biological effects of C5orf30 on the synovial fibroblasts, we used small interfering RNA technology (siRNA) to knockdown gene expression. RASF seeded at $2–5 \times 10^5$ cells per well (passages 3–6) were transfected with 50 nM C5orf30 or nontargeting control (NTC) smartpool siRNA by using Dharmafect 4 (Thermoscientific). The ON-Targetplus SMARTpool siRNA sequences for C5orf30 are CGAUUUAGGAGAGUCU, CUUCACGACUGGCGAGGAA, GUCAAUGGCAGGCGAA, and CUACCAUACGAGAUU. The cells were incubated at 37 °C and 5% CO_2 for 24–72 h. Immunofluorescence microscopy, radioactive proliferation, Western blotting, and real-time PCR assessed C5orf30 gene and protein expression.

C5orf30 Overexpression. RASF were transfected with 5 μg of pCMV6-Entry Vector (TrueORF clone; Origene) containing the ORF of C5orf30 and C-terminal Myc-DDK flag tag by using TurboFectin 8.0 (Origene) transfection reagent. Control cells were transfected with an empty vector or turbofectin only. Gel electrophoresis and real-time PCR was used to assess the effects of C5orf30 overexpression at the mRNA level. Western blotting was used to detect Myc-DDK tag by using anti-DKK monoclonal antibody (OTI4C5, Origene).

Immunofluorescence Staining. Frozen synovial tissue sections (5 μM) were fixed in 4% (vol/vol) paraformaldehyde and were incubated with mouse monoclonal antibodies against antifibroblast surface protein (Abcam IB10), CD3, CD19, CD31, Neutrophil elastase (AbD Serotec), or mature macrophages CD68 (PG-M1, DAKO) alone or coincubated with rabbit polyclonal anti-C5orf30 for 1 h followed by addition of Alexa Fluor 488-conjugated donkey anti-rabbit and Alexa Fluor 594-conjugated goat anti-mouse (Life Technologies). Of note, the anti-fibroblast antibody (IB10) may also detect

myeloid cells including monocytes and macrophages. Slides were placed in ProLong Gold anti-fade reagent mounting medium with 4′,6-diamidino-2-phenylindole (Invitrogen). Sections were also incubated for 1 h with an isotype-matched control, or normal rabbit serum (Dako) was used as negative controls. Images were collected by using a confocal microscope (LSM510; Zeiss). The background fluorescence level was set with the negative controls, and images were analyzed by using Zen image analysis software 2009 (Zeiss). The same staining protocol was used for immunofluorescence of primary RASF seeded onto chamber slides (Lab-Tek; Nunc) and fixed in 4% paraformaldehyde. To study C5orf30 localization within the cells, RASF were stained with anti-C5orf30 combined with mouse anti-β-actin or, anti-LAMP1 (Lysosome-Associated Membrane Protein 1) and processed as above. Each coverslip was mounted onto slides by using 30 μL of Hard Set Vector Shield and left to harden overnight. The slides were covered in foil to avoid light exposure and were visualized on a confocal fluorescence microscope.

Western Blotting. Whole-cell lysates from cultured RASF was prepared from 2×10^6 cells by homogenization in MPer Mammalian protein extraction buffer (ThermoScientific). A *C5orf30* overexpression lysate made from vector-transfected HEK293 cells was used as a positive control (Novus Biologicals). Protein samples were separated on 10% precast SDS/PAGE gels (Bio-Rad) and transferred onto a nitrocellulose membrane by using the iBlot machine Western blot transfer stacks (Life Technologies). The membrane was incubated with 5% skimmed milk in Tris-buffered saline (TBS) with 0.1% Tween 20 (TBS-T). The primary antibodies to C5orf30 and β-actin were diluted in milk/TBS-T and incubated for 2 h at room temperature. After washing with TBS-T, the hybridized bands were detected by using an enhanced chemiluminescence (ECL) detection kit and Hyperfilm-ECL reagents (Amersham Pharmacia). The membrane was viewed in the BioRad ChemiDoc XRS+ molecular imaging machine with Image Lab 4.0.1 software.

Invasion Assay. In vitro invasion of RASF was assayed in a transwell system by using the BD BioCoat BD Matrigel Invasion Chamber (BD Biosciences) as described (43). Briefly, RASF that has undergone C5orf30 knockdown were harvested by trypsin-EDTA digestion. Then 2.0×10^4 cells were resuspended in 500 μL of serum-free DMEM and plated in the upper compartment of the Matrigel-coated inserts. The lower compartment was filled with Complete media, and the plates were incubated at 37 °C for 24 h. The upper surface of the insert was then wiped with a cotton swab to remove noninvading cells and the Matrigel layer. The opposite side of the insert was stained with hematoxylin/eosin (Sigma), and the total number of cells that invaded through Matrigel were counted at 100× magnification. To assess the average number of migrating cells, cells were counted in five random high-power fields (*SI Methods*).

ACKNOWLEDGMENTS. Microarrays and computational analysis was carried out by Cambridge Genomic Services, and we thank Dr. Julien Bauer for his methodological advice. This work was supported by grants from the University of Sheffield and Arthritis Ireland.

1. Linn-Rasker SP, et al. (2006) Smoking is a risk factor for anti-CCP antibodies only in rheumatoid arthritis patients who carry HLA-DRB1 shared epitope alleles. *Ann Rheum Dis* 65(3):366–371.
2. Maxwell JR, Gowers IR, Moore DJ, Wilson AG (2010) Alcohol consumption is inversely associated with risk and severity of rheumatoid arthritis. *Rheumatology (Oxford)* 49(11):2140–2146.
3. Marinou I, Maxwell JR, Wilson AG (2010) Genetic influences modulating the radiological severity of rheumatoid arthritis. *Ann Rheum Dis* 69(3):476–482.
4. Knevel R, et al. (2012) Genetic predisposition of the severity of joint destruction in rheumatoid arthritis: A population-based study. *Ann Rheum Dis* 71(5):707–709.
5. Mewar D, et al. (2008) Association between radiographic severity of rheumatoid arthritis and shared epitope alleles: Differing mechanisms of susceptibility and protection. *Ann Rheum Dis* 67(7):980–983.
6. van der Linden MP, et al. (2009) Association of a single-nucleotide polymorphism in CD40 with the rate of joint destruction in rheumatoid arthritis. *Arthritis Rheum* 60(8): 2242–2247.
7. Knevel R, et al. (2012) Studying associations between variants in TRAF1-C5 and TNFAIP3-OLIG3 and the progression of joint destruction in rheumatoid arthritis in multiple cohorts. *Ann Rheum Dis* 71(10):1753–1755.
8. Krabben A, et al. (2013) Association of genetic variants in the IL4 and IL4R genes with the severity of joint damage in rheumatoid arthritis: A study in seven cohorts. *Arthritis Rheum* 65(12):3051–3057.
9. Knevel R, et al. (2012) Genetic variants in IL15 associate with progression of joint destruction in rheumatoid arthritis: A multicohort study. *Ann Rheum Dis* 71(10):1651–1657.
10. Stahl EA, et al.; BIRAC Consortium; YEAR Consortium (2010) Genome-wide association study meta-analysis identifies seven new rheumatoid arthritis risk loci. *Nat Genet* 42(6):508–514.
11. Viatte S, et al. (2012) Genetic markers of rheumatoid arthritis susceptibility in anti-citrullinated peptide antibody negative patients. *Ann Rheum Dis* 71(12):1984–1990.
12. Teare MD, et al. (2013) Allele-dose association of the C5orf30 rs26232 variant with joint damage in rheumatoid arthritis. *Arthritis Rheum* 65(10):2555–2561.
13. Wright KJ, et al. (2011) An ARL3-UNC119-RP2 GTPase cycle targets myristoylated NPHP3 to the primary cilium. *Genes Dev* 25(22):2347–2360.
14. Cen O, Gorska MM, Stafford SJ, Sur S, Alam R (2003) Identification of UNC119 as a novel activator of SRC-type tyrosine kinases. *J Biol Chem* 278(10):8837–8845.
15. Gorska MM, Stafford SJ, Cen O, Sur S, Alam R (2004) Unc119, a novel activator of Lck/Fyn, is essential for T cell activation. *J Exp Med* 199(3):369–379.
16. Müller-Ladner U, et al. (1996) Synovial fibroblasts of patients with rheumatoid arthritis attach to and invade normal human cartilage when engrafted into SCID mice. *Am J Pathol* 149(5):1607–1615.
17. Huerta-Cepas J, et al. (2011) PhylomeDB v3.0: An expanding repository of genome-wide collections of trees, alignments and phylogeny-based orthology and paralogy predictions. *Nucleic Acids Res* 39(Database issue):D556–D560.
18. Cole C, Barber JD, Barton GJ (2008) The Jpred 3 secondary structure prediction server. *Nucleic Acids Res* 36(Web Server issue):W197–W201.
19. Linding R, Russell RB, Neduva V, Gibson TJ (2003) GlobPlot: Exploring protein sequences for globularity and disorder. *Nucleic Acids Res* 31(13):3701–3708.
20. Dinkel H, et al. (2012) ELM–the database of eukaryotic linear motifs. *Nucleic Acids Res* 40(Database issue):D242–D251.
21. Obata T, et al. (2000) Peptide and protein library screening defines optimal substrate motifs for AKT/PKB. *J Biol Chem* 275(46):36108–36115.
22. Pawlus MR, Wang L, Ware K, Hu CJ (2012) Upstream stimulatory factor 2 and hypoxia-inducible factor 2α (HIF2α) cooperatively activate HIF2 target genes during hypoxia. *Mol Cell Biol* 32(22):4595–4610.
23. Brennan FM, et al. (1992) Enhanced expression of tumor necrosis factor receptor mRNA and protein in mononuclear cells isolated from rheumatoid arthritis synovial joints. *Eur J Immunol* 22(7):1907–1912.
24. Biniecka M, et al. (2010) Oxidative damage in synovial tissue is associated with in vivo hypoxic status in the arthritic joint. *Ann Rheum Dis* 69(6):1172–1178.
25. Bradfield PF, et al. (2003) Rheumatoid fibroblast-like synoviocytes overexpress the chemokine stromal cell-derived factor 1 (CXCL12), which supports distinct patterns and rates of CD4+ and CD8+ T cell migration within synovial tissue. *Arthritis Rheum* 48(9):2472–2482.
26. Kok SH, et al. (2013) Simvastatin inhibits cysteine-rich protein 61 expression in rheumatoid arthritis synovial fibroblasts through the regulation of sirtuin-1/FoxO3a signaling. *Arthritis Rheum* 65(3):639–649.
27. Kiener HP, et al. (2009) Cadherin 11 promotes invasive behavior of fibroblast-like synoviocytes. *Arthritis Rheum* 60(5):1305–1310.
28. Midwood K, et al. (2009) Tenascin-C is an endogenous activator of Toll-like receptor 4 that is essential for maintaining inflammation in arthritic joint disease. *Nat Med* 15(7): 774–780.
29. Haas CS, et al. (2006) Identification of genes modulated in rheumatoid arthritis using complementary DNA microarray analysis of lymphoblastoid B cell lines from disease-discordant monozygotic twins. *Arthritis Rheum* 54(7):2047–2060.
30. Courties G, et al. (2010) In vivo RNAi-mediated silencing of TAK1 decreases inflammatory Th1 and Th17 cells through targeting of myeloid cells. *Blood* 116(18):3505–3516.
31. Huber LC, et al. (2006) Synovial fibroblasts: Key players in rheumatoid arthritis. *Rheumatology (Oxford)* 45(6):669–675.
32. Zhang H, et al. (2011) UNC119 is required for G protein trafficking in sensory neurons. *Nat Neurosci* 14(7):874–880.
33. Pettersson M, Bessonova M, Gu HF, Groop LC, Jönsson JI (2000) Characterization, chromosomal localization, and expression during hematopoietic differentiation of the gene encoding Arl6ip, ADP-ribosylation-like factor-6 interacting protein (ARL6). *Genomics* 68(3):351–354.
34. Astro V, Chiaretti S, Magistrati E, Fivaz M, de Curtis I (2014) Liprin-α1, ERC1 and LL5 define polarized and dynamic structures that are implicated in cell migration. *J Cell Sci* 127(Pt 17):3862–3876.
35. Raj T, et al. (2014) Polarization of the effects of autoimmune and neurodegenerative risk alleles in leukocytes. *Science* 344(6183):519–523.
36. Zhang X, et al. (2015) Identification of common genetic variants controlling transcript isoform variation in human whole blood. *Nat Genet* 47(4):345–352.
37. Berkovits BD, Mayr C (2015) Alternative 3′ UTRs act as scaffolds to regulate membrane protein localization. *Nature* 522(7556):363–367.
38. Rantapää-Dahlqvist S, et al. (2003) Antibodies against cyclic citrullinated peptide and IgA rheumatoid factor predict the development of rheumatoid arthritis. *Arthritis Rheum* 48(10):2741–2749.
39. Klareskog L, Rönnelid J, Lundberg K, Padyukov L, Alfredsson L (2008) Immunity to citrullinated proteins in rheumatoid arthritis. *Annu Rev Immunol* 26:651–675.
40. Okada Y, et al.; RACI consortium; GARNET consortium (2014) Genetics of rheumatoid arthritis contributes to biology and drug discovery. *Nature* 506(7488):376–381.
41. Mewar D, Wilson AG (2011) Treatment of rheumatoid arthritis with tumour necrosis factor inhibitors. *Br J Pharmacol* 162(4):785–791.
42. Muthana M, et al. (2011) Use of macrophages to target therapeutic adenovirus to human prostate tumors. *Cancer Res* 71(5):1805–1815.
43. Ng CT, et al. (2010) Synovial tissue hypoxia and inflammation in vivo. *Ann Rheum Dis* 69(7):1389–1395.